Diamond & Related Materials 96 (2019) 52–57

Contents lists available at ScienceDirect

Diamond & Related Materials

journal homepage: www.elsevier.com/locate/diamond

Ultrasmall diamond nanoparticles with unusual incompressibility

Mikhail Popov[a,b,c,*], Valentin Churkin[a,c], Danila Ovsyannikov[a], Almaz Khabibrakhmanov[a,c], Alexey Kirichenko[a], Elena Skryleva[b], Yury Parkhomenko[b], Mikhail Kuznetsov[a], Sergei Nosukhin[a], Pavel Sorokin[a,b,c], Sergey Terentiev[a], Vladimir Blank[a,c]

[a] Technological Institute for Superhard and Novel Carbon Materials, 108840, 7a Tsentralnaya, Troitsk, Moscow, Russian Federation
[b] National University of Science and Technology MISiS, 119049, Leninskiy Prospect 4, Moscow, Russian Federation
[c] Moscow Institute of Physics and Technology State University, 141700, Institutskiy per. 9, Dolgoprudny, Moscow Region, Russian Federation

ARTICLE INFO

Keywords:
Nanodiamond
Raman spectroscopy
High pressure

ABSTRACT

Based on experimental and theoretical studies, the 607 GPa bulk modulus of nanodiamond 2–5 nm was determined, which significantly exceeds the bulk modulus of diamond crystal (443 GPa) and approaches the values typical of ultrahard fullerite (600–1000 GPa). Bulk modulus of nanodiamond 2–5 nm was experimentally measured by piezospectroscopy using a diamond anvil cell with anvils made of synthetic diamond with a high (~60%) ^{13}C isotope content. The Raman frequency in such diamond is at 1306 cm^{-1} and does not interfere with the recording of a peak at 1325 cm^{-1} of nanodiamond 2–5 nm. The bulk compression modulus was calculated from the dependence of the displacement of two Raman bands at 1325 cm^{-1} and 1600 cm^{-1} (the latter does not apply to sp^2 bonds) of nanodiamond 2–5 nm on pressure up to 68 GPa. Simulation of nanodiamond 1.2–5.9 nm confirms experimental results and also predicts the rise of bulk modulus with a decrease of nanoparticles size. Analysis of simulated structures suggests a possible explanation of observed effect due to increasing contribution of surficial compressed bonds when nanoparticles size reduces.

1. Introduction

The problem of creating materials that exceed the mechanical properties of diamond is widely discussed [1] (and references therein), starting with the calculation of bulk compression modulus of a single fullerene molecule (903 GPa) and a hypothetical material formed by C_{60} (668 GPa) [2,3], and the subsequent discovery of ultrahard fullerite, [4] which has an even higher bulk compression modulus (from 500 to 1000 GPa, depending on the structure and synthesis conditions) [5].

One of the problems with the explanation of specific properties of such materials is that they lack the translational order at distances greater than 1–2 nm [5]. C_{60} cluster is a molecule with icosahedral symmetry which is not compatible with translational symmetry and there are no associated crystallographic point or space groups. Consequently, a long-term periodicity of a high-density crystal lattice (for example, hcp or fcc) could not be possible for the covalently bonded C_{60} molecules in three dimensions (3D C_{60}). At the same time, theoretical calculations for hypothetical unbounded crystal structures of 3D C_{60} show bulk compression moduli lower than diamond [6,7] (and references therein). Reducing the size of the 3D C_{60} clusters to 1–2 nm (surrounded by a 1–3 nm diamond matrix) allows one to obtain a designed bulk modulus above 1000 GPa [1].

Another feature of ultrahard fullerite is the presence of 70% sp^3 bonds, according to X-ray photoelectron spectroscopy (XPS) [8]. Thus, from the viewpoint of creating materials that surpass diamond in mechanical properties, it is interesting to trace how the properties of diamond change as the grain size decreases. We should highlight the following feature of diamond. At temperatures below ~1000–1300 K (below the Debye temperature), dislocation plasticity is practically absent in diamond [9], and diamond is one of the few materials whose strength is equal to the 55 GPa theoretical yield limit [9,5]. For comparison, in germanium and silicon, theoretical yield limit can hardly be achieved despite the absence of dislocation plasticity at temperatures below the Debye temperature. The fact is that a phase transition already begins in these materials at stresses lower than the theoretical yield limit (which, in turn, is the mechanism of plastic deformation) [9]. Diamond is unique in the context of its theoretical yield limit being simultaneously equal to the experimental value of its yield limit [5], shear stress at which the diamond lattice loses stability and the phase transition begins [10] and also equal to the stress at which dislocation movement begins [9]. Consequently, the strength (and, respectively,

* Corresponding author at: Technological Institute for Superhard and Novel Carbon Materials, 108840, 7a Tsentralnaya, Troitsk, Moscow, Russian Federation.
E-mail address: mikhail.popov@tisnum.ru (M. Popov).

https://doi.org/10.1016/j.diamond.2019.04.033
Received 13 February 2019; Received in revised form 25 April 2019; Accepted 29 April 2019
Available online 01 May 2019
0925-9635/ © 2019 Elsevier B.V. All rights reserved.

hardness) of diamond is determined by its elastic modulus.

As a result, the Hall-Petch effect is absent in diamond (an increase in strength with decreasing grain size, which is typical for materials with dislocation plasticity) with grain sizes larger than 5 nm. Indeed, a diamond indenter leaves indents on nanocrystalline samples [11,12,13,14] which is direct evidence that the indenter material hardness (diamond single crystal) is higher than the hardness of the tested sample (polycrystalline diamond with a grain size larger than 10–20 nm). For comparison, the Knoop diamond indenter does not scratch [15] even the softest (100) diamond face (albeit in the "hardest" [110] direction on this face) of a nitrogen-free diamond. Only an indenter made of ultra-hard fullerite can make indents on all faces, including the hardest (111) face, in a diamond crystal [5,16].

A decrease in the grain size below 5 nm leads to a significant increase in the diamond bulk modulus B_0 from 443 GPa (bulk crystal) to 564 GPa (nanoparticle) [17]. In Ref. [17] it was shown that the Raman spectra of 2–5 nm nanodiamonds are characterized by bands at 1325 cm^{-1} and 1600 cm^{-1} (the latter, as shown in [17] does not apply to sp^2 bonds) and 1500 cm^{-1} (which shifts to 1630 cm^{-1} when changing 458 nm laser excitation to 257 nm). The diamond nanoparticles bulk modulus was measured by piezospectroscopy using the 1600 cm^{-1} band displacement under pressure up to 50 GPa implementing a diamond anvil cell (DAC) [17]. Due to the high bulk modulus, the band at 1325 cm^{-1} is hidden by the Raman spectrum of the diamond anvil. The point is that the singlet mode ω_s of the stressed anvil tip depends on the pressure in the sample P as $\partial\omega_s/\partial P = 2.24\ cm^{-1}$/GPa [18]. Raman band $\omega = 1333\ cm^{-1}$ of a single-crystal diamond shifts under pressure as $\partial\omega/\partial P = 2.90\ cm^{-1}$/GPa (above ~50 GPa, the dependence noticeably deviates from the linear). Therefore, one can observe the Raman spectrum of a single-crystal diamond compressed in a DAC using a hydrostatic pressure-transmitting medium. In accordance with the value of $B_0 = 564$ GPa for diamond nanoparticles, the $\omega = 1325\ cm^{-1}$ band dependence on the pressure should be $\partial\omega/\partial P = 2.2\ cm^{-1}$/GPa, $\omega = 1325\ cm^{-1}$, i.e. it will always be hidden by the Raman spectrum of the diamond anvil, in contrast with a single-crystal diamond [17].

Since the reason for the appearance of the 1600 cm^{-1} band in diamond nanoparticles has not been precisely determined yet, the definition of the modulus B_0 only from the displacement of this band is not fully correct. Therefore, in an experimental study of the bulk compression modulus of diamond nanoparticles by piezospectroscopy, we used diamond anvils made of synthetic diamond with a high (~60%) ^{13}C isotope content. The Raman frequency shift in such a diamond is 1306 cm^{-1} and does not interfere with the recording of a 1325 cm^{-1} peak characteristic for nanodiamonds. We also carried out a simulation of diamond nanoparticles in 1.2–5.9 nm size region. Experimental and simulation data showed that the bulk modulus of diamond nanoparticles sufficiently exceeds bulk modulus of diamond crystal.

2. Experimental and theoretical methods

We used a DAC for the high-pressure study. Experimental anvils in the DAC were made of IIa synthetic diamonds with a high ^{13}C isotope content. Diamonds were grown under high pressure and temperature conditions using a temperature gradient method at the Technological Institute for Superhard and Novel Carbon Materials, Troitsk, Moscow, Russian Federation. The Raman frequency of the grown diamonds is 1306 cm^{-1}, which corresponds to a content of approximately ~60% of the ^{13}C isotope [19].

As diamond nanoparticles, we used a detonation 2–5 nm diamond produced by the SINTA company (**Republic of Belarus**). According to a procedure described in Ref. [17], the nanodiamond was treated in a planetary mill with a mixture of 25 wt% of NaCl for removing the rest of the contamination layers. A mixture of diamond nanoparticles and NaCl (which in this case plays the role of a hydrostatic pressure-transmitting medium) was loaded into a prepared hole in a tungsten gasket. Transmission electron microscope (TEM) study was done by a JEM 2010 high-resolution microscope (JEOL Ltd., Tokyo, Japan). During preparation of the sample for TEM study, NaCl was removed by a solution in a mixture of water and ethanol.

The Raman spectra were recorded with a TRIAX 552 (Jobin Yvon Inc., Edison, NJ) spectrometer, equipped with a CCD Spec-10, 2KBUV Princeton Instruments 2048 × 512 detector and razor edge filters (excitation wavelength was 405 nm) and a Renishaw inVia Raman microscope (excitation wavelength 532 nm).

The pressure was measured both on the ruby pressure scale [20] and from the stress-induced shifts of the Raman spectra from the diamond anvil [18]. Since we used diamond anvils made of synthetic diamond with a high content of ^{13}C isotope, we performed an additional calibration of the diamond pressure scale using the technique described in Ref. [18] to a pressure of 60 GPa. In contrast to the natural isotopic composition (~99% of ^{12}C), the singlet mode ω_s of the stressed diamond (~60% of ^{13}C) anvil tip depends on the pressure in the sample P as $\partial\omega_s/\partial P = 1.66(\pm 0.05)\ cm^{-1}$/GPa within measurement accuracy. For the anvil with natural isotopic composition, $\partial\omega_s/\partial P = 2.24(\pm 0.05)\ cm^{-1}$/GPa.

X-ray Photoelectron Spectroscopy (XPS) measurements were performed on a PHI 5000 VersaProbe II spectrometer with a monochromatic focused AlKα radiation ($h\nu = 1486.6$ eV) operated at 50 W. A dual beam charge compensation system was used to provide neutralization of charge at the sample surface. The analysis was carried out on the raw surface of the samples and after Ar^+ 2 keV ion irradiation during 5 min (9 nm/min sputter rate, determined for SiO_2 film) performed to remove the adsorbed contaminants.

For a theoretical study of the atomic structure and mechanical properties of the proposed models of nanodiamonds, modified Tersoff potential [21] was used (implemented into a LAMMPS package [22]) which allows consideration of systems consisting from thousands to millions of atoms. The undoubted advantage of this method is the possibility of modeling a large system with a sufficiently high calculating speed. To evaluate the accuracy of the chosen approach, the cell parameters and elastic properties of bulk diamond were calculated. Modified Tersoff potential allows to predict the structural parameters of bulk diamond with an error less than 0.1% (compared to the experimental data taken from Ref. [23]: $a_{Tersoff} = 3.565$ Å, $a_{exp} = 3.568$ Å). The bulk modulus of diamond was determined as $B_0^{Tersoff} = 445$ GPa which corresponds well with the experimental values of 445 GPa [5] and 442 GPa [24].

3. Results and discussion

Raman spectra of the diamond nanoparticles loaded at different pressures in a DAC with anvils of ~60% ^{13}C are shown in Fig. 1. For comparison, Fig. 1 provides the Raman spectrum of diamond nanoparticles loaded to a pressure of 51 GPa in a DAC with anvils of ~99% ^{12}C. The Raman spectra of the ~99% ^{12}C anvil completely hide the 1325 cm^{-1} line of diamond nanoparticles Raman spectra (which shifts to 1442 cm^{-1} under pressure of 51 GPa). The Raman line of a hydrostatically loaded "bulk" diamond under a pressure of 51 GPa would be located at a frequency of ~1481 cm^{-1} [25].

Raman spectra presented in Fig. 2 with the exception of the spectrum at 56 GPa were recorded with the 405 nm excitation wavelength; the spectrum at 56 GPa was recorded with the 532 nm excitation wavelength. When Raman spectra were excited by a 405 nm laser, the luminescence level was significantly lower than when excited at 532 nm.

Fig. 2 illustrates, for comparison, the Raman spectra taken from the gasket and from the sample at a pressure of 26 GPa. Since the 1325 cm^{-1} line of diamond nanoparticles is fairly close to the Raman spectrum of the ~60% ^{13}C diamond anvil (under pressure of 26 GPa, their position is 1381 and 1349 cm^{-1}, respectively), at pressures below 40 GPa this line is seen as a shoulder to a more intense line from the anvil. However, when normalizing the spectrum of the sample to the

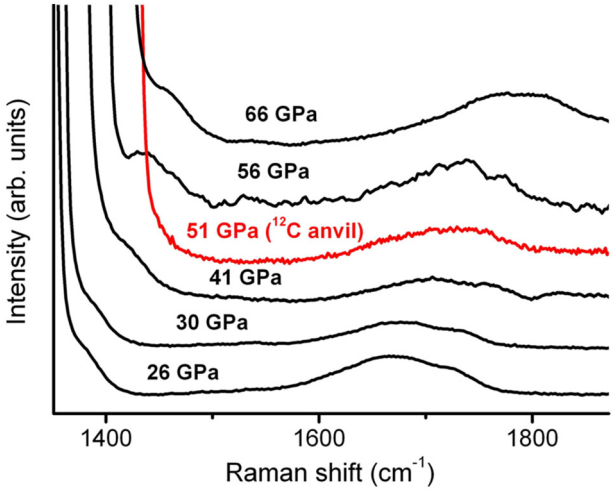

Fig. 1. Raman spectrum of diamond nanoparticles loaded at different pressures in a DAC with anvils of ~60% of ^{13}C (the lower spectrum). For comparison, the Raman spectrum of diamond nanoparticles loaded to a pressure of 51 GPa in a DAC with anvils of ~99% of ^{12}C is shown. Raman spectra of the ~99% ^{12}C anvil completely hide the 1325 cm^{-1} line of Raman spectra of diamond nanoparticles.

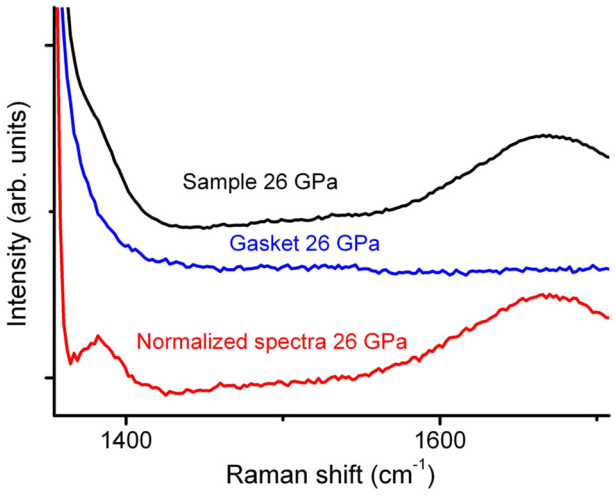

Fig. 2. Raman spectra taken from the gasket and from the sample at a 26 GPa pressure, and normalized spectra of the sample.

spectrum taken from the gasket (by subtracting the latter from the former), the Raman band of diamond nanoparticles is well resolved (normalized spectra, Fig. 2).

Raman spectra of the sample (diamond nanoparticles which mixed with NaCl) after the pressure treatment did not change (Fig. 3) even after an irradiation under pressure of 66 GPa by a 15 mW laser beam with a 532 nm wavelength focused to a 1–2 μm spot in steps of 2 μm for 100 s in each position exactly as in Ref. [26,27]. This is an essential feature of diamond nanoparticles which shows stability under pressure above 55 GPa contrary to nanodiamond 25 nm. Indeed, nanodiamond 25 nm transforms into onion-type structures in the pressure range 55–115 GPa under the laser irradiation during Raman spectra acquisition [26,27]. Accordingly, diamond Raman band disappears at pressure 55 GPa and D and G bands of amorphous carbon are observed in the sample upon pressure release [26,27]. Along this nanodiamond 25 nm is characterized by a typical for diamond bulk modulus 443 GPa [17].

TEM study of diamond nanoparticles before (Fig. 4a) and after (Fig. 4b) the pressure (66 GPa) treatment shows no changes in a structure as well as the Raman study.

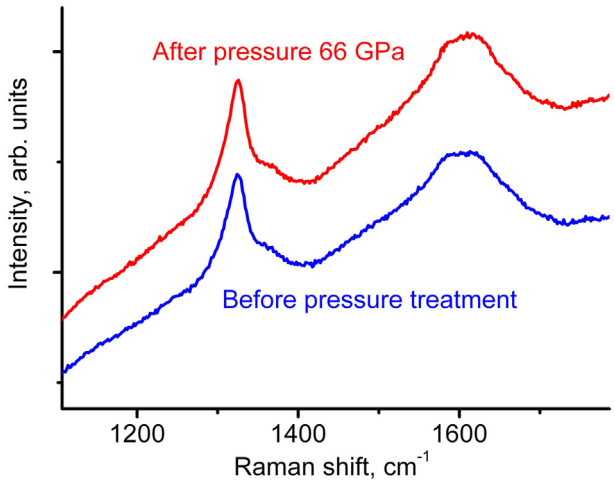

Fig. 3. Raman spectra before (bottom) and after pressure treatment (upper). The excitation wavelength is 405 nm.

According to the dependence of the Raman lines on pressure, one can determine the bulk modulus taking into account the known relation [28].

$$\gamma_i = \frac{\partial \ln \omega_i}{\partial \ln V} = \frac{B_0}{\omega_0}\frac{\partial \omega_i}{\partial P} \quad (1)$$

Here γ_i is the Gruneisen parameter for a quasiharmonic mode of frequency ω_i (ω_0 marks the one at zero pressure, B_0 is bulk modulus). In general, $\gamma \approx 1$ for covalently bonding group IV semiconductors [28], and in particular $\gamma = 0.96$ for diamond [25].

Fig. 5 presents the experimental data on the relative Raman shift $(\omega-\omega_0)/\omega_0$ (relative frequency) for diamond nanoparticles with $\omega_0 = 1325\ \text{cm}^{-1}$ (marked with triangles) and with $\omega_0 = 1600\ \text{cm}^{-1}$ (marked with circles). The latter, as shown in [17] does not apply to sp^2 bonds. As can be seen from Fig. 5, the relative frequencies of these two lines are almost the same. This gives grounds to combine the data for both frequencies with $\omega_0 = 1325\ \text{cm}^{-1}$ and $\omega_0 = 1600\ \text{cm}^{-1}$. Least-squares fit line (with a $1.59 \times 10^{-3}\ \text{GPa}^{-1}$ slope) for the combined data is shown in Fig. 5. For comparison, there is a straight line (with a $2.18 \times 10^{-3}\ \text{GPa}^{-1}$ slope), corresponding to the dependence of the relative frequency on pressure for a diamond single crystal with $\omega_0 = 1333\ \text{cm}^{-1}$, corresponding to the dependence $\partial\omega/\partial P = 2.9\ \text{cm}^{-1}/\text{GPa}$ [25].

Comparing the slopes of the straight lines shown in Fig. 5, in accordance with formula (1), we obtain the bulk modulus for the diamond nanoparticles $B_0 = 607 \pm 20$ GPa. For comparison, in [17] a close bulk modulus value of diamond nanoparticles (564 GPa) was calculated only from the $\omega_0 = 1600\ \text{cm}^{-1}$ line dependence on pressure.

The features of the electronic structure of 2–5 nm diamond nanoparticles are also manifested in the XPS spectra of carbon. When comparing the C1s spectra of single diamond crystal, 250 nm diamond and 2–5 nm diamond nanoparticles, see Fig. 6, we observe differences in the shape of the peaks.

On the initial surface of the samples, this difference is manifested in a significant broadening of the peak for nanodiamonds (the half-width of the half-height line HWHH C1s is 0,75 eV in the single diamond crystal, 1.2 eV in 250 nm diamond and 2.5 eV in 2–5 nm diamond nanoparticles), which is associated with a decrease in the degree of structure ordering. After cleaning the samples in situ with Ar^+ ions with an energy of 2 keV for 5 min, we observe a different structure of the C1s peaks, which is the result of adsorbed hydrocarbons removal on the one hand, and partial graphitization of the samples with an ion beam on the other hand. In the 250 nm nanodiamond sample (as well as in the single diamond crystal), we see two peaks shifted relative to each other on the scale of binding energy (BE) by differential charging: an

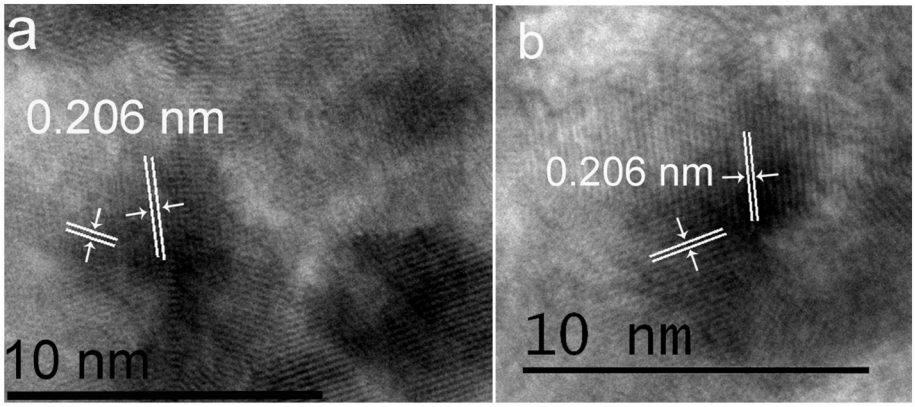

Fig. 4. TEM study of diamond nanoparticles before (Fig. 4a) and after (Fig. 4b) the pressure (66 GPa) treatment. The distances between the {111} planes are 0.206 nm and angle between these planes is 70° (110°).

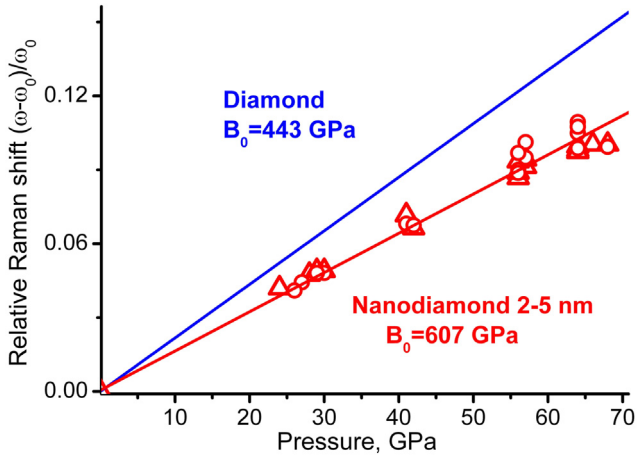

Fig. 5. Experimental data on the relative Raman shift $(\omega-\omega_0)/\omega_0$ (relative frequency) dependence on pressure for diamond nanoparticles with $\omega_0 = 1325\,cm^{-1}$ (marked with triangles) and with $\omega_0 = 1600\,cm^{-1}$ (marked with circles; one as shown in [17] does not apply to sp^2 bonds) and their least-squares fit line. For comparison, there is a straight line corresponding to the relative frequency dependence on pressure for a diamond single crystal with $\omega_0 = 1333\,cm^{-1}$.

asymmetric peak 1 (284.5 eV) from sp^2-bound atoms and a symmetric peak 2 (285.7 eV) from sp^3-bound atoms. In a 2–5 nm diamond nanoparticles sample, this C1s spectrum structure typical for using monochromatic X-ray radiation is complicated by the appearance of an additional peak in the region of 287 eV. Low oxygen concentration (less than 1.5 at. %) does not allow attributing this peak to oxygen bonds, so there can be only one explanation: additional charge differentiation, which can be associated with the presence of diamond nanoparticles with higher dielectric properties than large 250 nm diamond crystals.

In order to elucidate reasons of diamond nanoparticles stiffening, we investigated their mechanical properties theoretically in the wide size region. According to experimental conditions, diamond nanoparticles are located in a solid medium which allows assuming that their surface is chemically bonded and therefore it shouldn't undergo reconstruction. Full atomic structure relaxation of single diamond nanoparticles showed the absence of surface reconstruction; surface bond angles were preserved nearly the same as those of bulk diamond. For this reason, nanodiamonds can be considered as consisting of fully sp^3-hybridized atoms with surficial dangling bonds which represent a chemical connection with the medium. Due to the full sp^3-hybridization of the nanodiamonds, we chose the nanoparticles' shape to be a cubic one according to the reference prediction [29] of the most stable shape of fully passivated diamond nanoclusters. The studied diamond nanoparticles have their cube edge length, d, in a range from 1.2 to 5.9 nm.

We characterized the mechanical properties of the considered structures by their bulk modulus B_0. Bulk modulus describes the ability of a material to change its volume under the influence of uniform hydrostatic compression. To get the energy vs. volume curve required for bulk modulus calculations, each relaxed structure was hydrostatically compressed and expanded. At each step, surface carbon atoms were frozen, whereas the rest of the atoms were fully relaxed. Based on the calculated data, the energy of each investigated structure depending on its volume was evaluated, and bulk modulus of all considered structures was found using the Birch-Murnaghan equation [30]. The volume of the structure was determined as the volume of a convex hull of nanodiamond atoms without taking into account atomic radii of the surficial atoms. This is not the only possible definition of a volume for nanoparticle, but we chose it as the most explicit and well-formalized one.

Obtained dependence of bulk modulus upon the diamond nanoparticles size is presented in Fig. 7a (blue diamonds). The pronounced increasing of the B_0 with the structure size reduction coincides with the experimental observation, whereas with nanodiamonds enlarging, B_0 approaches to the corresponding value for bulk diamond. The origin of the studied structures ultrastiffness can be understood by the analysis of bond lengths in optimized structures. Color distribution of bond lengths in diamond nanoparticles of two sizes is shown in Fig. 7b and c. As it can be seen, the surface and near-surface bonds are shorter than in bulk diamond (1.46–1.53 Å) and as soon as shorter bonds are stronger, they mainly contribute to the stiffening of the diamond nanoparticle. On the other hand, the minor presence of elongated bonds (1.56–1.62 Å) cannot significantly affect the resulting nanostructure stiffness. Therefore, in total nanodiamonds become more incompressible than bulk diamond.

Such a conclusion can be proved by estimation of the B_0 as the normalized sum over the atomic bulk moduli. Due to a localized character of chemical bonds in diamond, its B_0 is directly linked to the mechanical stiffness of bonds. The concept of atomic bulk modulus was developed by Kleovoulou et al. [31] and further used in theoretical works [1,32] where the investigation of local rigidity in carbon and silicon nanostructures was performed. In our case bond lengths of each atom in the nanoparticle were averaged which allowed associating with each atom the value of the local bulk modulus equal to the bulk modulus of diamond crystal with the same bond length. Using the values of local bulk moduli, the total B_0 of the nanoparticle could be found as their normalized sum. Indeed, the dependence of diamond crystal bulk modulus on the lattice constant (and therefore bond length) shows the evident increase with the bonds shortening (see the inset in Fig. 7a), so the studied nanoparticles with contracted bonds on the surface should be more rigid than diamond crystal. The obtained dependence of bulk

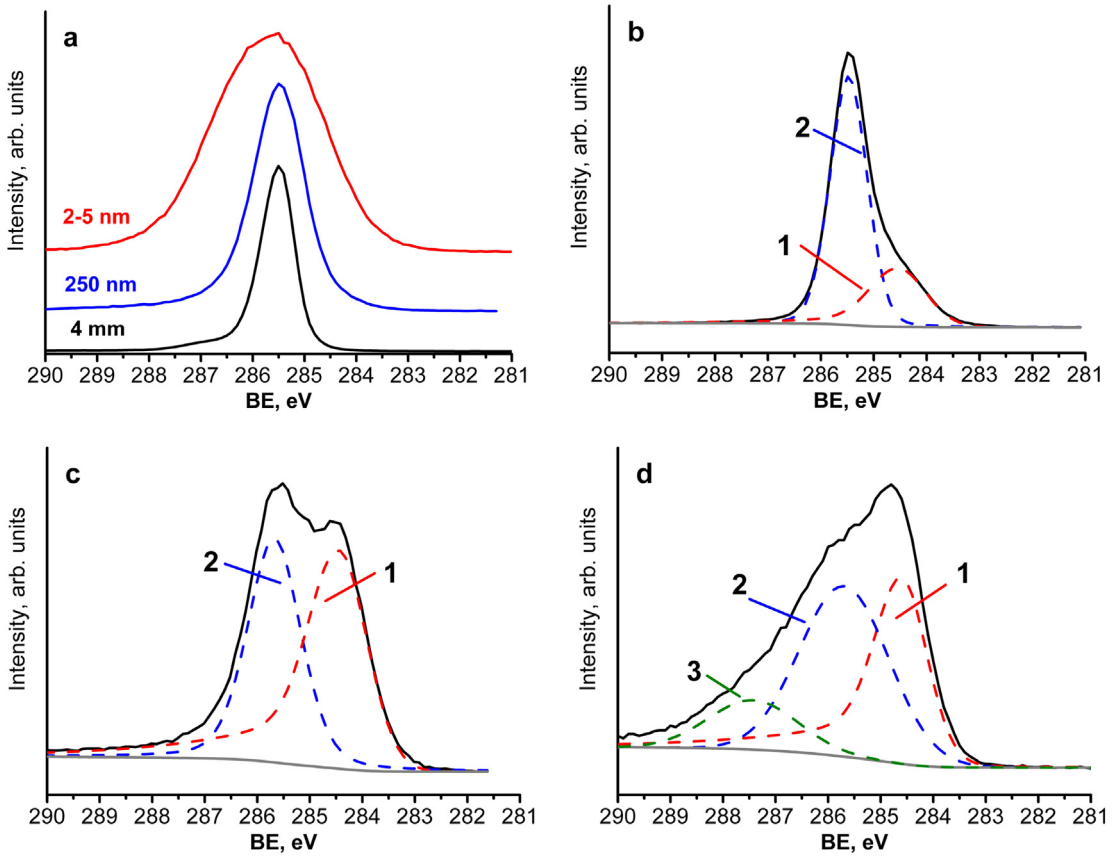

Fig. 6. XPS Spectra C1s of single diamond crystal (type IIa, face (111), size of the face 4 × 4 mm), 250 nm diamond and 2–5 nm diamond nanoparticles on the initial surface of the samples (a) and after sputtering by an Ar^+ (2 keV) ion beam of the single diamond crystal (b), 250 nm diamond sample (c) and a 2–5 nm diamond nanoparticles sample (d).

modulus calculated as the normalized sum over the atomic bulk moduli (Fig. 7a, red circles) shows close correlation with directly calculated B_0 which ensures that the observed effect is mostly originated from the surface bonds contraction. Obtained dependences can be well fitted by inverse law ($1/d$) which additionally reflects the dominant surface contribution to the observed effect.

4. Conclusions

Based on experimental and theoretical studies, we determined the diamond nanoparticles bulk modulus as equal to 607 ± 20 GPa. Both Raman lines of diamond nanoparticles with $\omega_0 = 1325\ cm^{-1}$ and with $\omega_0 = 1600\ cm^{-1}$ were observed up to the maximum pressure of 68 GPa within this study. The dependences of the relative frequencies on the pressure of these two lines practically coincide. Diamond nanoparticles simulations suggest that observed high bulk modulus is originated from the compressed bonds in the near-surface region. This conclusion is also supported by the growth of bulk modulus inversely proportional to nanodiamonds size.

Acknowledgements

This work was supported by the Russian Foundation for Basic Research (project 18-29-19019); the part of theoretical calculations (design of diamond nanoparticles) work was supported by a grant of the Russian Science Foundation (project #16-12-10293); the work was

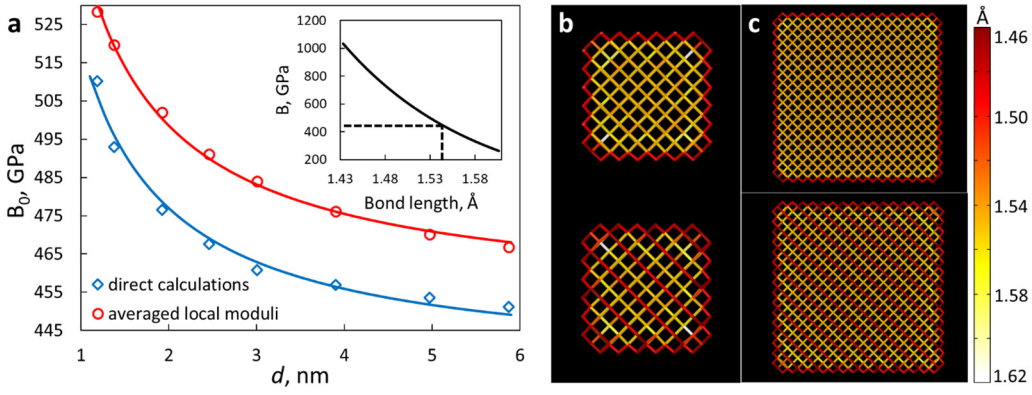

Fig. 7. Results of the theoretical investigation. (a) Size-dependence of nanodiamonds bulk modulus calculated in an explicit way (blue diamonds) and estimated as the normalized sum over the atomic bulk moduli (red circles). Obtained data were fitted by the hyperbolic curves. In the inset, the dependence of diamond crystal bulk modulus on the bond length is presented. Values of B_0 (relaxed state) and corresponding bond length are marked by dashed lines. (b–c) Bond length color distribution in diamond nanoparticles with diameter $d = 1.2$ nm (b) and $d = 3.0$ nm (c) viewed from [100] direction, respectively. Top and bottom sections correspond to nanoparticle's middle slice and surface, respectively. The dominance of contracted bonds over lengthened ones is explicit.

done using the Shared Research Facilities “Research of Nanostructured, Carbon and Superhard Materials” FSBI TISNCM and Joint Research Center “Material Science and Metallurgy” NUST MISiS. We are grateful to the supercomputer cluster provided by the Materials Modelling and Development Laboratory at NUST “MISIS” (supported via the Grant from the Ministry of Education and Science of the Russian Federation No. 14.Y26.31.0005) and to the Joint Supercomputer Center of the Russian Academy of Sciences. We thank Viktor Denisov and Vladimir Denisov for assistance in Raman spectra recording.

References

[1] Y.A. Kvashnina, A.G. Kvashnin, M.Y. Popov, B.A. Kulnitskiy, I.A. Perezhogin, E.V. Tyukalova, L.A. Chernozatonskii, P.B. Sorokin, V.D. Blank, Toward the Ultra-incompressible Carbon Materials. Computational Simulation and Experimental Observation, J. Phys. Chem. Lett., 6 (2015) 2147-2152.
[2] R.S. Ruoff, A.L. Ruoff, Is C60 stiffer than diamond? Nature 350 (1991) 663–664.
[3] R.S. Ruoff, A.L. Ruoff, The bulk modulus of C60 molecules and crystals: A molecular mechanics approach, Appl. Phys. Lett. 59 (1991) 1553–1555.
[4] V. Blank, M. Popov, S. Buga, V. Davydov, V. Agafonov, R. Ceolin, H. Szwarc, A. Rassat, Is C 60 fullerite harder than diamond? Physics Letters A 188 (1994) 281–286.
[5] M. Popov, B. Kulnitskiy, V. Blank, Superhard materials, based on fullerenes and nanotubes. In Comprehensive Hard Materials, 515–538, ed. V. Sarin. 2014 Elsevier. 1800.
[6] J. Yang, J.S. Tse, T. Iitaka, First-principles Investigation on the Geometry and Electronic Structure of the Three-dimensional Cuboidal C60 Polymer, J. Chem. Phys. 127 (2007) 134906.
[7] S. Berber, E. Osawa, D. Tománek, Rigid Crystalline Phases of Polymerized Fullerenes, Phys. Rev. B 70 (2004) 085417.
[8] Yu.N. Parkhomenko, E.A. Skrileva, B.L. Sanakoev, V.D. Blank, B.A. Kulnitskiy, G.A. Dubitsky, N.R. Serebryanaya, S.G. Buga. Carbon bonds hybridization in fullerites studied by XPS. in Nanotechnologies in the Area of Physics, Chemistry and Biotechnology. Fifth ISTC Scientific Advisory Committee Seminar 2002. St-Petersburg Russia.
[9] J.J. Gilman, Chemistry and Physics of Mechanical Hardness, John Wiley & Sons, Inc, 2009.
[10] M. Popov, Stress-induced phase transition in diamond, High Pressure Research 30 (2010) 670–678.
[11] H. Tang, X. Yaan, P. Yu, Q. Hu, M. Wang, Y. Yao, L. Wu, Q. Zou, Y. Ke, Y. Zhao, L. Wang, X. Li, W. Yang, H. Gou, H.-k. Maof, W.L. Mao, Revealing the formation mechanism of ultrahard nanotwinned diamond from onion carbon, Carbon 129 (2018) 159–167.
[12] Q. Huang, D. Yu, B. Xu, W. Hu, Y. Ma, Yanbin Wang, Z. Zhao, B. Wen, J. He, Z. Liu, Y. Tian, Nanotwinned diamond with unprecedented hardness and stability, Nature, 510 (2014) 250-253.
[13] N. Dubrovinskaia, L. Dubrovinsky, F. Langenhorst, S. Jacobsen, C. Liebske, Nanocrystalline diamond synthesized from C60, Diamond and Related Materials 14 (2005) 16–22.
[14] T. Irifune, A. Kurio, S. Sakamoto, T. Inoue, H. Sumiya, Materials: ultrahard polycrystalline diamond from graphite, Nature 421 (2003) 599–600.
[15] H. Sumiya, N. Toba, S. Satoch, Mechanical properties of synthetic type IIa diamond crystal, Diamond Relat. Mater. 6 (1997) 1841–1846.
[16] V. Blank, M. Popov, G. Pivovarov, N. Lvova, K. Gogolinsky, V. Reshetov, Ultrahard and superhard phases of fullerite C60: comparison with diamond on hardness and wear, Diamond and Related Materials, 7 (1998) 427-431.
[17] M. Popov, V. Churkin, A. Kirichenko, V. Denisov, D. Ovsyannikov, B. Kulnitskiy, I. Perezhogin, V. Aksenenkov, V. Blank, Raman spectra and bulk modulus of nanodiamond in a size interval of 2-5 nm. Nanoscale Research Letters, 12 (2017) 561 (1-6).
[18] M. Popov, Pressure measurements from Raman spectra of stressed diamond anvils, J. Appl. Phys. 95 (2004) 5509–5514.
[19] M. Cardona, M.L.W. Thewalt, Isotope effects on the optical spectra of semiconductors, Rev. Mod. Phys. 77 (2005) 1173–1224.
[20] K. Syassen, Ruby under pressure, High Pressure Research 28 (2008) 75–126.
[21] P. Erhart, K. Albe, Analytical potential for atomistic simulations of silicon, carbon, and silicon carbide, Physical Review B 71 (2005) 035211.
[22] S. Plimpton, Fast parallel algorithms for short-range molecular dynamics, Journal of Computational Physics 117 (1995) 1–19.
[23] V.D. Blank, V.V. Aksenenkov, M.Y. Popov, S.A. Perfilov, B.A. Kulnitskiy, Y.V. Tatyanin, O.M. Zhigalina, B.N. Mavrin, V.N. Denisov, A.N. Ivlev, V.M. Chernov, V.A. Stepanov, A new carbon structure formed at MeV neutron irradiation of diamond: structural and spectroscopic investigations, Diamond and Related Materials 8 (1999) 1285–1290.
[24] M. Cohen, Calculation of bulk moduli of diamond and zinc-blende solids, Physical Review B 32 (1985) 7988–7991.
[25] M. Hanfland, K. Syassen, S. Fahy, S.G. Louie, M.L. Cohen, Pressure dependence of the first-order Raman mode id diamond, Phys. Rev. B 31 (1985) 6896–6899.
[26] Vladimir D. Blank, Valentin D. Churkin, Boris A. Kulnitskiy, Igor A. Perezhogin, Alexey N. Kirichenko, Viktor N. Denisov, Sergey V. Erohin, Pavel B. Sorokin, M.Y. Popov, Phase diagram of carbon and the factors limiting the quantity and size of natural diamonds, Nanotechnology, 29 (2018) 115603
[27] Vladimir D. Blank, Valentin D. Churkin, Boris A. Kulnitskiy, Igor A. Perezhogin, Alexey N. Kirichenko, Sergey V. Erohin, Pavel B. Sorokin, M.Y. Popov, Pressure-induced transformation of graphite and diamond to onions, Crystals, 8 (2018) 68 (1-8).
[28] B.A. Weinstein, R. Zallen, Pressure-Raman Effects in Covalent and Molecular Solids. Light Scattering in Solids, ed. M.C.a.G. Guntherodt. Vol. IV. 1984, Berlin, Springer. 543.
[29] A.S. Barnard, P. Zapol, A model for the phase stability of arbitrary nanoparticles as a function of size and shape, The Journal of Chemical Physics 121 (2004) 4276–4283.
[30] F. Birch, Finite elastic strain of cubic crystals, Physical Review B 71 (1947) 809–824.
[31] K. Kleovoulou, P.C. Kelires, Stress state of embedded si nanocrystals, Phys. Rev. B 88 (2013) 085424.
[32] K. Kleovoulou, P.C. Kelires, Local rigidity and physical trends in embedded Si nanocrystals, Phys. Rev. B 88 (2013) 245202.